

# Sommerfeld Enhancements for Asymmetric Dark Matter

Aerman Sulitan, Hoernisa Iminniyaz, Mu Baoxia\*

*School of Physics Science and Technology, Xinjiang University,  
Urumqi 830046, China*

## Abstract

We extend the analysis of asymmetric Dark Matter relic density with Sommerfeld enhancement to the case where the mediator is massive. In asymmetric Dark Matter models, the asymmetric Dark Matter is assumed to couple to light scalar or vector boson. Asymmetric Dark Matter annihilation cross section is enhanced by the Sommerfeld effect which exists due to the distortion of wavefunction of asymmetric Dark Matter particle and anti-particle by long-range interactions. The impacts of Sommerfeld enhancement on the relic densities of asymmetric Dark Matter particle and anti-particle are discussed. The effect of kinetic decoupling on the relic density is also probed when the annihilation cross section is enhanced by Sommerfeld enhancement. Finally, the constraints on the parameter space is given by using the observational data of Dark Matter.

arXiv:2009.13410v1 [hep-ph] 28 Sep 2020

---

\*Corresponding author, wrns@xju.edu.cn

# 1 Introduction

The astrophysical and cosmological observations show that most of the matter in the universe is dark. The nature of Dark Matter (DM) is not known to us although we have the precise value for DM relic density from the observations [1]. One assumption is that DM maybe asymmetric [2, 3, 4]. The idea of asymmetric DM arises from the hypothesis that the present day abundance of DM may have the same origin with the visible or ordinary matter. The motivations come from the fact that the present day DM density is about 5 times of the average density of baryons  $\Omega_{\text{DM}} \simeq 5\Omega_b$ .

In asymmetric DM models, it is often assumed that DM couples to light or massless force carriers [4, 5, 6, 7, 8]. If the mediator is light enough, the interaction between the asymmetric DM particle and anti-particle is appeared as long-range. The wavefunctions of asymmetric DM particles and anti-particles are distorted by the long-range interaction if asymmetric DM interacts via the exchange of light mediators. It is the well-known Sommerfeld effect which enhances the annihilation cross section of asymmetric DM particle and anti-particle [9]. The Sommerfeld enhancement has effect on the relic density of asymmetric DM at some level.

In ref.[10], the authors explored the effect of Sommerfeld enhancement on the relic densities of asymmetric DM particle and anti-particle for  $m_\phi = 0$ . In ref.[10], the Sommerfeld enhancement factor  $S_0$  is approximated by its value at  $m_\phi = 0$ ,  $S_0 = \pi\alpha/v/(1 - e^{-\pi\alpha/v})$ , where  $v$  is the velocity of asymmetric DM particle and anti-particle in the center-of-mass frame,  $\alpha$  is the coupling strength. They obtained the result that the anti-particle abundance is significantly affected by the Sommerfeld effect comparing to the particle abundance. The decrease of abundance depends on the coupling strength  $\alpha$ . The impact of kinetic decoupling on the relic abundance of asymmetric DM is also analyzed when the annihilation cross section is changed by the Sommerfeld enhancement in ref.[10].

In refs.[11, 12], the relic density of symmetric DM is discussed when the light mediator mass  $m_\phi \neq 0$ , where  $m_\phi \ll m$  with  $m$  being the DM mass. In our work, we extend this exploration to the asymmetric DM case. For massive mediator, the Sommerfeld enhancement is saturated at low velocity, and exhibits resonant behavior at some specific values of  $m_\phi$  [13]. Sommerfeld enhancement boosts the late-time DM annihilation signals [14, 15]. The coupling of asymmetric DM to the light force mediator determines the Sommerfeld enhancement. The coupling for asymmetric DM needs to be stronger than the symmetric DM of the same mass. Therefore, the importance of Sommerfeld enhancement for the phenomenology of asymmetric DM may be more significant than the symmetric DM case. We investigate the quantitative impact of Sommerfeld enhancement on the asymmetric DM relic density for the case of  $m_\phi \neq 0$ . When the asymmetric DM particles and anti-particles decoupled from the

chemical equilibrium, they were still in kinetic equilibrium for a while due to the scattering of standard model particles. The background radiation temperature and the temperatures of asymmetric DM particle and anti-particle are different before and after kinetic decoupling [16, 17]. This difference leads to significant change of the relic density of asymmetric DM after kinetic decoupling. It results that the relic density of asymmetric DM is continuously decreased until the Sommerfeld enhancement is saturated at low velocity. The decrease is more sizable for asymmetric DM anti-particle than the particle. In our work, we only consider the Sommerfeld enhancement and neglect the effect of bound state formation on the relic density of asymmetric DM. The bound-state formation affects the relic density of DM only around the unitarity bound [8, 18].

The paper is arranged as following. In section 2, we discuss the effect of Sommerfeld enhancement on the asymmetric DM abundance. In section 3, we use the Planck data to obtain the constraints on parameter spaces. The last section is devoted to the conclusions.

## 2 Effect of Sommerfeld enhancement on the asymmetric DM abundance

Asymmetric DM annihilation process may be due to the long-range interactions mediated by light mediator. If asymmetric DM couples to light force mediator, the wavefunction of asymmetric DM particle and anti-particle is distorted by the long-range interaction. It is the Sommerfeld effect [9]. This results the annihilation cross section of asymmetric DM is enhanced at low velocity. The Sommerfeld enhanced annihilation cross section affects the relic density of asymmetric DM.

When the mediator mass  $m_\phi \neq 0$ , the analytic approximation of the Sommerfeld enhancement factor for  $s$ -wave annihilation [19, 20, 11, 12] is

$$S = \frac{\pi}{\epsilon_v} \frac{\sinh\left(\frac{2\pi\epsilon_v}{\pi^2\epsilon_\phi/6}\right)}{\cosh\left(\frac{2\pi\epsilon_v}{\pi^2\epsilon_\phi/6}\right) - \cos\left(2\pi\sqrt{\frac{1}{\pi^2\epsilon_\phi/6} - \frac{\epsilon_v^2}{(\pi^2\epsilon_\phi/6)^2}}\right)}, \quad (1)$$

where  $\epsilon_v \equiv v/\alpha$  and  $\epsilon_\phi \equiv m_\phi/(\alpha m)$ . For  $\epsilon_\phi \gg \epsilon_v$ , there are resonances at

$$m_\phi \simeq \frac{6\alpha m}{\pi^2 n^2}, \quad (2)$$

here  $n$  is the positive integer. The Sommerfeld enhancement factor for low  $v$  is  $S \simeq \pi^2\alpha m_\phi/(6mv^2)$  at these resonances with  $m_\phi$  given by Eq.(2).

Following, we discuss the impact of Sommerfeld enhancement on the relic densities of asymmetric DM particle and anti-particle in model independent way. Usually it is assumed

the asymmetric DM particles and anti-particles were in thermal equilibrium with the standard model particles in the radiation dominated universe. When the annihilation rate  $\Gamma_{\text{an}} = n_{\chi, \bar{\chi}} \langle \sigma v_{\text{rel}} \rangle$  is less than the expansion rate  $H$ , the particles and anti-particles can not keep in the chemical equilibrium and decouple from thermal plasma. Here,  $n_{\chi, \bar{\chi}}$  are the number densities of asymmetric DM particle  $\chi$  and anti-particle  $\bar{\chi}$ ,  $\langle \sigma v_{\text{rel}} \rangle$  is the thermal average of the annihilation cross section  $\sigma$  multiplied with the relative velocity  $v_{\text{rel}}$  of asymmetric DM particle and anti-particle,  $v = v_{\text{rel}}/2$ . The temperature at which the decoupling occurred is called freeze out temperature. The asymmetric DM abundance is almost fixed at the freeze out temperature [21, 22, 23]. To determine the relic density  $\Omega_{\text{DM}}$  of DM, we need to solve the Boltzmann equations which describe the particle and anti-particle evolution in the universe.

The Boltzmann equations expressed by the ratio of  $n_{\chi, \bar{\chi}}$  to entropy density  $s$ ,  $Y_{\chi, \bar{\chi}} = n_{\chi, \bar{\chi}}/s$  with  $s = 2\pi^2 g_{*s}/45 T^3$ , are

$$\frac{dY_{\chi}}{dx} = -\frac{\langle \sigma v_{\text{rel}} \rangle s}{Hx} (Y_{\chi} Y_{\bar{\chi}} - Y_{\chi, \text{eq}} Y_{\bar{\chi}, \text{eq}}), \quad (3)$$

$$\frac{dY_{\bar{\chi}}}{dx} = -\frac{\langle \sigma v_{\text{rel}} \rangle s}{Hx} (Y_{\chi} Y_{\bar{\chi}} - Y_{\chi, \text{eq}} Y_{\bar{\chi}, \text{eq}}), \quad (4)$$

where  $x = m/T$ , and the expansion rate is  $H = \pi T^2 \sqrt{g_*/90}/M_{\text{Pl}}$ , here  $g_{*s}$ ,  $g_*$  are the effective number of entropic degrees of freedom and relativistic degrees of freedom.  $M_{\text{Pl}} = 2.4 \times 10^{-18} \text{GeV}$  is the reduced Planck mass. Here we assume only the asymmetric Dark Matter particle  $\chi$  and anti-particle  $\bar{\chi}$  annihilate into standard model particles. Thermal average of the Sommerfeld enhanced annihilation cross section is

$$\langle \sigma v_{\text{rel}} \rangle = \sigma_0 \langle S(v_{\text{rel}}) \rangle, \quad (5)$$

here  $\sigma_0$  corresponds to the s-wave annihilation cross section,

$$\langle S(v_{\text{rel}}) \rangle = \frac{x^{3/2}}{2\sqrt{\pi}} \int_0^{\infty} v_{\text{rel}}^2 e^{-\frac{x}{4} v_{\text{rel}}^2} S dv_{\text{rel}}. \quad (6)$$

The equilibrium abundances for the asymmetric DM particle and anti-particle are

$$Y_{\chi, \text{eq}} = \frac{90}{(2\pi)^{7/2}} \frac{g_{\chi}}{g_{*s}} x^{3/2} e^{-x(1-\mu_{\chi}/m)}, \quad (7)$$

$$Y_{\bar{\chi}, \text{eq}} = \frac{90}{(2\pi)^{7/2}} \frac{g_{\chi}}{g_{*s}} x^{3/2} e^{-x(1+\mu_{\chi}/m)}, \quad (8)$$

where we used the fact that chemical potential  $\mu_{\bar{\chi}} = -\mu_{\chi}$  in equilibrium state, and  $g_{\chi}$  is the number of intrinsic degrees of freedom of the particle. Subtracting Eq.(4) from Eq.(3), we obtain  $dY_{\chi}/dx - dY_{\bar{\chi}}/dx = 0$ . This requires  $Y_{\chi} - Y_{\bar{\chi}} = \eta$ , where  $\eta$  is a constant. Then the Boltzmann equations are rewritten as

$$\frac{dY_{\chi}}{dx} = -\frac{\lambda \langle S(v_{\text{rel}}) \rangle}{x^2} (Y_{\chi}^2 - \eta Y_{\chi} - Y_{\text{eq}}^2), \quad (9)$$

$$\frac{dY_{\bar{\chi}}}{dx} = -\frac{\lambda \langle S(v_{\text{rel}}) \rangle}{x^2} (Y_{\bar{\chi}}^2 + \eta Y_{\bar{\chi}} - Y_{\text{eq}}^2), \quad (10)$$

here  $Y_{\text{eq}}^2 = Y_{\chi, \text{eq}} Y_{\bar{\chi}, \text{eq}} = (0.145 g_{\chi}/g_*)^2 x^3 e^{-2x}$  and  $\lambda = 1.32 m M_{\text{Pl}} \sigma_0 \sqrt{g_*}$ , where we assume  $g_* \simeq g_{*s}$  and  $dg_*/dx \simeq 0$ .

Eqs.(9) and (10) can be solved numerically. We can also obtain the semi-analytical solution by repeating the same method which is used in ref.[22]. First, we can have the semi-analytic result of Eq.(10). We use the deviation  $\Delta_{\bar{\chi}} = Y_{\bar{\chi}} - Y_{\bar{\chi}, \text{eq}}$  to express the Boltzmann equation (10) as

$$\Delta'_{\bar{\chi}} = -Y'_{\bar{\chi}, \text{eq}} - \lambda x^{-2} \langle S(v_{\text{rel}}) \rangle \Delta_{\bar{\chi}} (2Y_{\bar{\chi}, \text{eq}} + \Delta_{\bar{\chi}} + \eta), \quad (11)$$

here  $\prime$  denotes  $d/dx$  and  $Y_{\bar{\chi}, \text{eq}} = -\eta/2 + \sqrt{\eta^2/4 + Y_{\text{eq}}^2}$ , which is obtained by using the fact that right hand side of equation (4) vanishes in equilibrium. When the temperature is high, the value of  $Y_{\bar{\chi}}$  tracks its equilibrium value very closely, and  $\Delta^2$  and  $\Delta'$  are negligible. Then we obtain

$$\Delta_{\bar{\chi}} \simeq \frac{2x^2 Y_{\text{eq}}^2}{\lambda \langle S(v_{\text{rel}}) \rangle (\eta^2 + 4Y_{\text{eq}}^2)}. \quad (12)$$

The Sommerfeld effect is not significant up to the time of freeze out, therefore we use standard method to fix the freeze out temperature. The freeze out temperature is defined as following,

$$\Delta_{\bar{\chi}, \text{ns}}(\bar{x}_f) = \xi Y_{\bar{\chi}, \text{eq}}(\bar{x}_f), \quad (13)$$

where  $\Delta_{\bar{\chi}, \text{ns}}(\bar{x}_f) \simeq 2\bar{x}_f^2 Y_{\text{eq}}^2 / [\lambda(\eta^2 + 4Y_{\text{eq}}^2)]$ , which is indeed Eq.(12) without including Sommerfeld factor, here  $\bar{x}_f$  is the freeze out temperature for asymmetric DM anti-particle, it results

$$2\bar{x}_f^2 Y_{\text{eq}}^2 / [\lambda(\eta^2 + 4Y_{\text{eq}}^2)] = \xi Y_{\bar{\chi}, \text{eq}}(\bar{x}_f), \quad (14)$$

and  $\xi = \sqrt{2} - 1$  [23].  $\bar{x}_f$  is determined by iteratively solving Eq.(14).

For low temperature,  $Y_{\bar{\chi}, \text{eq}}$  is negligible. Dropping the terms related to  $Y_{\bar{\chi}, \text{eq}}$ , then Eq.(11) becomes

$$\Delta'_{\bar{\chi}} = -\lambda x^{-2} \langle S(v_{\text{rel}}) \rangle \Delta_{\bar{\chi}} (\Delta_{\bar{\chi}} + \eta). \quad (15)$$

Although the asymmetric DM particles and anti-particles decoupled from the chemical equilibrium, they were still in kinetic equilibrium for a while due to the scattering of the standard model particles. When the particles and anti-particles were in chemical and kinetic equilibrium, the temperatures  $T_{\chi, \bar{\chi}}$  of asymmetric DM track the background radiation temperature  $T$ ,  $T_{\chi, \bar{\chi}} = T$ . After kinetic decoupling, the temperatures of asymmetric DM particle and anti-particle scale as  $T_{\chi, \bar{\chi}} = T^2/T_k$ , where  $T_k$  is the kinetic decoupling temperature [16, 17, 24, 25]. The change of temperature of asymmetric DM before and after kinetic decoupling leaves its impact on the relic density of asymmetric DM. With the kinetic decoupling,

the thermal average of Sommerfeld enhancement factor takes the form as

$$\langle S_k(v_{\text{rel}}) \rangle = \frac{x^3}{2\sqrt{\pi} x_k^{3/2}} \int_0^\infty v_{\text{rel}}^2 e^{-\frac{x^2}{4x_k} v_{\text{rel}}^2} S dv_{\text{rel}}, \quad (16)$$

where  $x_k = m/T_k$ .

Integrating Eq.(15), we obtain the relic abundance of asymmetric DM anti-particle. The integration range should be separated into two parts after including kinetic decoupling: the first part is for the era before kinetic decoupling, the second part is for the era of after kinetic decoupling, then

$$Y_{\bar{\chi}}(x_s) = \eta \left\{ \exp \left[ 1.32 \eta m M_{\text{Pl}} \sigma_0 \sqrt{g_*} \left( \int_{\bar{x}_f}^{x_k} \frac{\langle S(v_{\text{rel}}) \rangle}{x^2} dx + \int_{x_k}^{x_s} \frac{\langle S_k(v_{\text{rel}}) \rangle}{x^2} dx \right) \right] - 1 \right\}^{-1}, \quad (17)$$

here  $x_s$  is the point at which the Sommerfeld enhancement saturates at low velocity. We assume that  $\Delta_{\bar{\chi}}(\bar{x}_f) \gg \Delta_{\bar{\chi}}(x_s)$ .

The asymmetric DM particle abundance is obtained by using the relation  $Y_\chi - Y_{\bar{\chi}} = \eta$ ,

$$Y_\chi(x_s) = \eta \left\{ 1 - \exp \left[ -1.32 \eta m M_{\text{Pl}} \sigma_0 \sqrt{g_*} \left( \int_{x_f}^{x_k} \frac{\langle S(v_{\text{rel}}) \rangle}{x^2} dx + \int_{x_k}^{x_s} \frac{\langle S_k(v_{\text{rel}}) \rangle}{x^2} dx \right) \right] \right\}^{-1}, \quad (18)$$

where  $x_f$  is the inverse scaled freeze out temperature for  $\chi$ . Eqs.(17) and (18) are only consistent with the constraint  $Y_\chi - Y_{\bar{\chi}} = \eta$  if  $x_f = \bar{x}_f$ .

The final DM relic density is given by

$$\Omega_{\text{DM}} h^2 \simeq 2.76 \times 10^8 m [Y_\chi(x_s) + Y_{\bar{\chi}}(x_s)], \quad (19)$$

where  $h = 0.673 \pm 0.098$  is the scaled Hubble constant in units of  $100 \text{ km s}^{-1} \text{ Mpc}^{-1}$  and  $\Omega_\chi = \rho_\chi/\rho_c$ . Here  $\rho_\chi = n_\chi m = s_0 Y_\chi m$  and the critic density is  $\rho_c = 3H_0^2 M_{\text{Pl}}^2$ , where  $s_0 \simeq 2900 \text{ cm}^{-3}$  is the present entropy density and  $H_0$  is the Hubble constant.

We use the numerical solutions of equations (9), (10) to plot the evolution of asymmetric DM abundance as a function of the inverse-scaled temperature  $x$  for  $\alpha = 0.02$  and  $\alpha = 0.1$  in Fig.1. Here  $\eta = 5 \times 10^{-13}$  in panels (a) and (b),  $\eta = 1 \times 10^{-12}$  in (c) and (d). The two thick and dashed (red) lines are for the asymmetric DM particle and anti-particle abundances without Sommerfeld enhancement; the dotted and dash-dotted (black) lines are the abundances of  $Y_\chi$  and  $Y_{\bar{\chi}}$  with Sommerfeld enhancement when the coupling strength  $\alpha = 0.02$  in (a), (c),  $\alpha = 0.1$  in (b), (d); the dashed (blue) line is for the equilibrium value of anti-particle abundance. Here  $m_\phi = 0.25 \text{ GeV}$ . The annihilation cross section is enhanced because of the Sommerfeld effect. The abundances of asymmetric DM particle and anti-particle are decreased due to the enhanced annihilation cross section. The size of the decrease depends on coupling strength

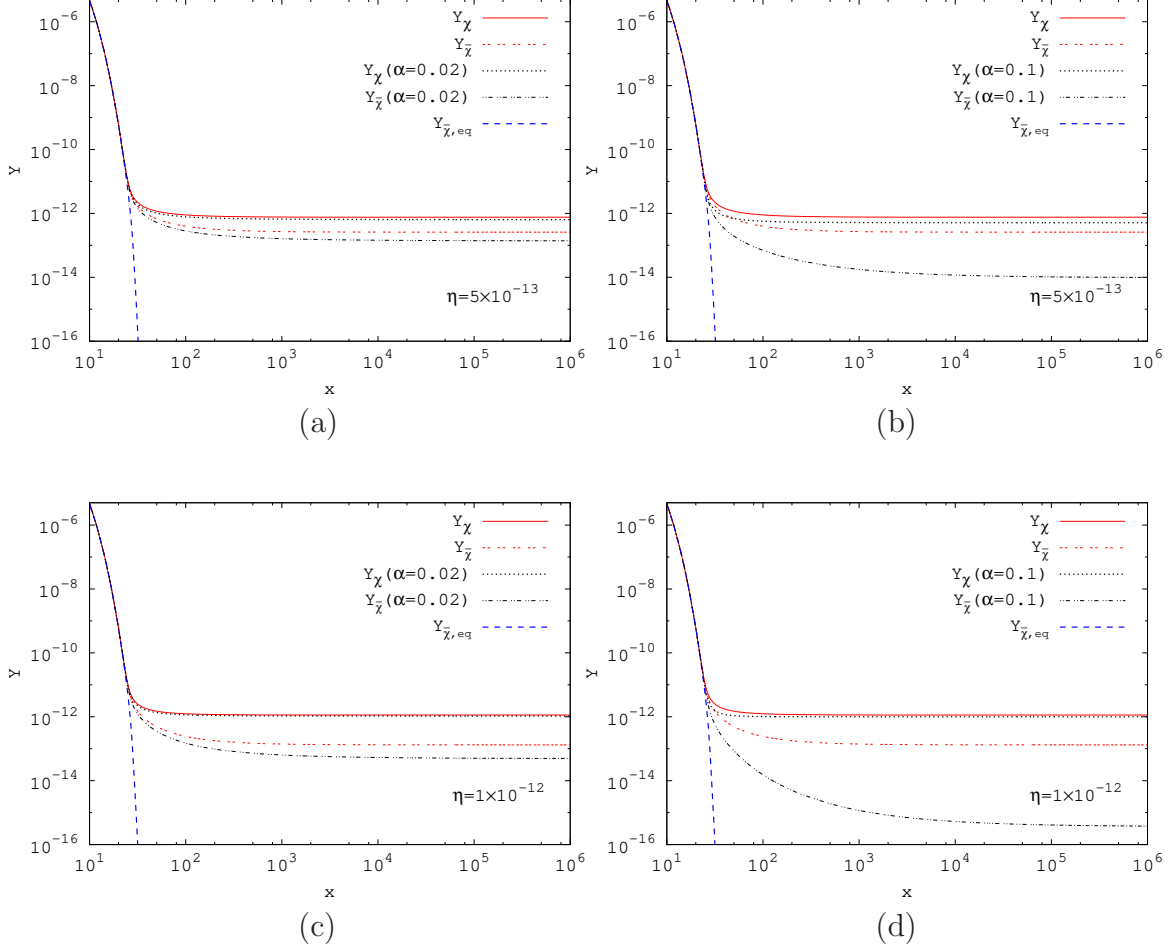


Figure 1: Asymmetric DM abundances  $Y_\chi$  and  $Y_{\bar{\chi}}$  as a function of  $x$  for the Sommerfeld enhanced annihilation cross section. Here  $\sigma_0 = 4 \times 10^{-26} \text{ cm}^3 \text{ s}^{-1}$ ,  $m = 500 \text{ GeV}$ ,  $x_f = 25$ ,  $m_\phi = 0.25 \text{ GeV}$ ,  $g_\chi = 2$ ,  $g_* = 90$ .

$\alpha$ . For example, the decreases of abundances  $Y_\chi$  and  $Y_{\bar{\chi}}$  are larger for  $\alpha = 0.1$  in panel (b), (d) than the case of  $\alpha = 0.02$  in (a), (c) in Fig.1. The reduction of anti-particle abundance is significant for larger coupling strength comparing to the case of particle abundance. When the asymmetry factor is smaller as  $5 \times 10^{-13}$ , the difference of asymmetric DM particle abundance with and without Sommerfeld enhancement is visible which is shown in panel (b) of Fig.1. For larger asymmetry factor as  $1 \times 10^{-12}$ , the decrease of particle abundance is not visible.

The relic abundances of asymmetric DM with Sommerfeld enhancement including the effect of kinetic decoupling is plotted in Fig.2 for  $\alpha = 0.02$  and  $\alpha = 0.1$ . These plots are based on the numerical solutions of equation (9), (10) with the separated integration range. The integration ranges are from  $x_f$  to  $x_k$  when there is only Sommerfeld enhancement and from  $x_k$  to  $x_s$  while there is kinetic decoupling. Here  $\eta = 1 \times 10^{-12}$ . The dotted (black) line is for anti-particle DM abundance for  $x_k = 10x_f$  and dashed (black) line is for  $x_k = 5x_f$ . We found the relic abundance of asymmetric DM anti-particle is continuously decreased after kinetic

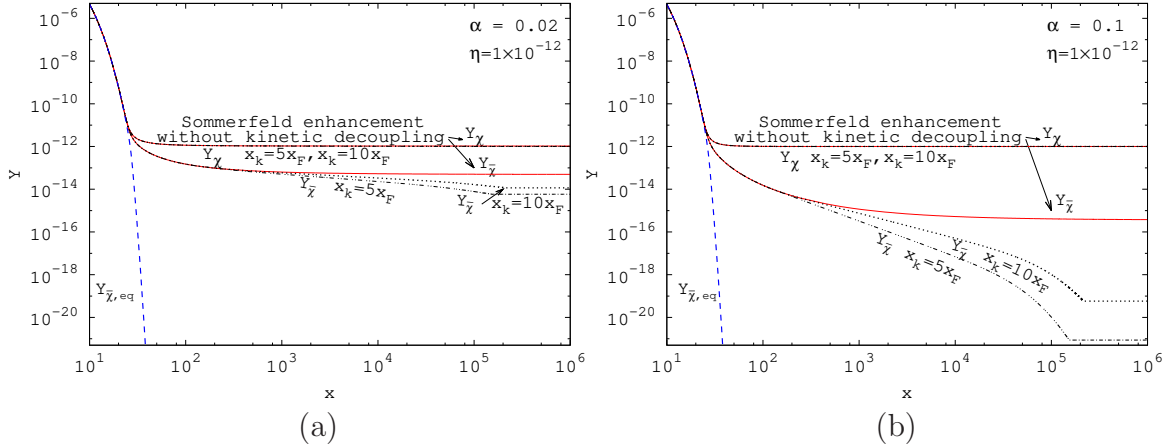


Figure 2: Evolution of  $Y$  for the particle and anti-particle as a function of  $x$  for the case when there is Sommerfeld enhancement with kinetic decoupling. Here  $\sigma_0 = 4 \times 10^{-26} \text{ cm}^3 \text{ s}^{-1}$ ,  $m = 500 \text{ GeV}$ ,  $x_f = 25$ ,  $m_\phi = 0.25 \text{ GeV}$ ,  $g_\chi = 2$ ,  $g_* = 90$ .

decoupling. When the kinetic decoupling temperature is closer to the freeze out temperature, the decrease is larger. In panel (a), around  $x = 1.5 \times 10^5$  for  $x_k = 5x_f$  and  $x = 2.5 \times 10^5$  for  $x_k = 10x_f$ , the curves become completely flat. It means  $Y_{\bar{\chi}}$  is constant. At this point, Sommerfeld enhancement is saturated. We can see the reason from Fig.3. When the velocity is small, the Sommerfeld factor  $S$  goes to constant value. This is the reason why  $Y_{\bar{\chi}}$  becomes constant. Here we take  $\alpha = 0.02$ ,  $m_\phi = 0.25 \text{ GeV}$ ,  $m = 500 \text{ GeV}$  in Fig.3. We took the parameter set in the paper where the Sommerfeld enhancement is not near a resonance. In panel (b), anti-particle abundance becomes stable from  $x = 1.6 \times 10^5$  for  $x_k = 5x_f$  and  $x = 2.2 \times 10^5$  for  $x_k = 10x_f$ . The decrease of asymmetric DM particle abundances are almost invisible in these plots. Asymmetric DM particle abundances for the two cases are overlapped with the case of without kinetic decoupling.

### 3 Constraints

We have the Planck data which provides the Dark Matter relic density as [1],

$$\Omega_{\text{DM}} h^2 = 0.1199 \pm 0.0022. \quad (20)$$

The contour plot of  $s$ -wave annihilation cross section  $\sigma_0$  and asymmetry factor  $\eta$  is shown in Fig.4 when  $\Omega_{\text{DM}} h^2 = 0.1199$ . The dotted (black) line is for the case of no Sommerfeld enhancement; long-dashed (blue) and double dot-dashed (black) lines correspond to the case of Sommerfeld enhancement without and with kinetic decoupling for  $\alpha = 0.02$ ; thick (red) and dot-dashed (red) lines are for  $\alpha = 0.1$ , here  $x_k = 5x_F$ . We found the required annihilation



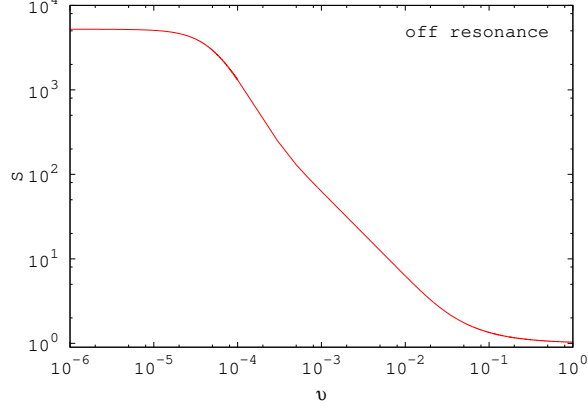


Figure 3: Sommerfeld enhancement factor  $S$  as a function of the velocity  $v$  for  $\alpha = 0.02$ ,  $m_\phi = 0.25$  GeV,  $m = 500$  GeV.

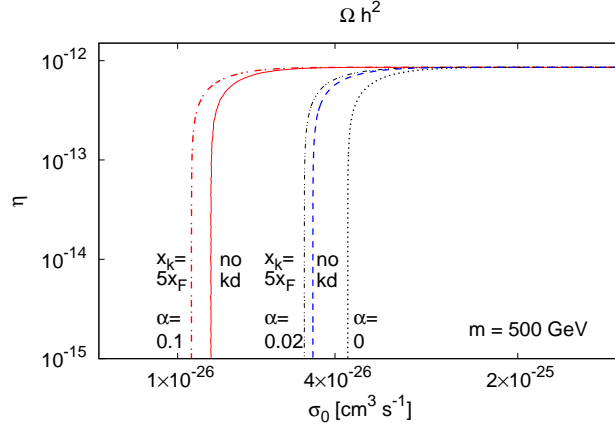


Figure 4: Contour plot of  $s$ -wave annihilation cross section  $\sigma_0$  and asymmetry factor  $\eta$  when  $\Omega_{\text{DM}}h^2 = 0.1199$ . Here  $m = 500$  GeV,  $x_f = 25$ ,  $m_\phi = 0.25$  GeV,  $g_\chi = 2$ ,  $g_* = 90$ .

cross section with the Sommerfeld enhancement is smaller than the case of without. There is less relic density due to the enhanced cross section. Therefore, the needed cross section should be smaller in order to satisfy the observed range of DM relic density. When there is kinetic decoupling, the required annihilation cross section is smaller than the case of no kinetic decoupling. The relic density of asymmetric DM is continuously decreased after the kinetic decoupling until the Sommerfeld enhancement saturates at small velocities. It results the required cross section for kinetic decoupling is smaller than the case of no kinetic decoupling when the asymmetry factor is small. For larger asymmetry factor, the required cross sections with kinetic decoupling and without are the same. The relic density is only determined by the asymmetry factor in that case.

## 4 Summary and conclusions

The effect of Sommerfeld enhancement on the relic density of asymmetric DM is discussed in this work. Here we generalize the case of massless force mediator to the massive case. The cross section between the asymmetric DM particle and anti-particle is enhanced by the Sommerfeld effect. We investigate in which extent the relic densities of asymmetric DM particle and anti-particle are affected when the asymmetric DM annihilation cross section is enhanced by the Sommerfeld effect. We found the asymmetric DM particle and anti-particle abundances are decreased due to the enhancement of annihilation cross section. The reduction of anti-particle relic abundance is more significant than particle abundance. The decrease depends on the size of coupling strength  $\alpha$ . For larger coupling strength, the decrease is larger.

After asymmetric DM particles and anti-particles decoupled from the chemical equilibrium, they were still in kinetic equilibrium for a while because of the scattering off relativistic standard model particles in the thermal plasma. The asymmetric DM particles and anti-particles decouple from the kinetic equilibrium when the scattering rate falls below the expansion rate. In our work, we explore the effects of kinetic decoupling on the relic density when there is Sommerfeld enhancement. We found the relic abundances of asymmetric DM are decreased continuously until the Sommerfeld enhancement saturates. The reduction of anti-particle abundance is significant than the particle abundance. The level of decrease depends on the kinetic decoupling temperature, coupling strength  $\alpha$ . For example, there is larger decrease when the kinetic decoupling temperature is more close to the freeze out point.

Finally, using the observed DM abundance, we obtain the constraints on the annihilation cross section and asymmetry factor when there is Sommerfeld enhancement. We found the required annihilation cross section with Sommerfeld enhancement is smaller than the case of without. Also the wanted annihilation cross section is smaller for the case of kinetic decoupling than the case of no kinetic decoupling. Those results are significant for asymmetric DM when Sommerfeld effect is important at low velocity. Sommerfeld effect implies notable indirect detection signals from asymmetric DM anti-particle. Therefore, we have the possibility to explore the asymmetric DM by the observation of CMB (Cosmic Microwave Background), the Milky way and Dwarf galaxies.

## Acknowledgments

The work is supported by the National Natural Science Foundation of China (11765021).

## References

- [1] P. A. R. Ade *et al.* [Planck Collaboration], *Astron. Astrophys.* **594**, (2016) A13 [arXiv:1502.01589 [astro-ph.CO]].
- [2] S. Nussinov, *Phys. Lett. B* **165**, (1985) 55; K. Griest and D. Seckel. *Nucl. Phys. B* **283**, (1987) 681; R. S. Chivukula and T. P. Walker, *Nucl. Phys. B* **329**, (1990) 445; D. B. Kaplan, *Phys. Rev. Lett.* **68**, (1992) 742; D. Hooper, J. March-Russell and S. M. West, *Phys. Lett. B* **605**, (2005) 228 [arXiv:hep-ph/0410114]; *JCAP* **0901** (2009) 043 [arXiv:0811.4153v1 [hep-ph]]; H. An, S. L. Chen, R. N. Mohapatra and Y. Zhang, *JHEP* **1003**, (2010) 124 [arXiv:0911.4463 [hep-ph]]; T. Cohen and K. M. Zurek, *Phys. Rev. Lett.* **104**, (2010) 101301 [arXiv:0909.2035 [hep-ph]]. D. E. Kaplan, M. A. Luty and K. M. Zurek, *Phys. Rev. D* **79**, (2009) 115016 [arXiv:0901.4117 [hep-ph]]; T. Cohen, D. J. Phalen, A. Pierce and K. M. Zurek, *Phys. Rev. D* **82**, (2010) 056001 [arXiv:1005.1655 [hep-ph]]; J. Shelton and K. M. Zurek, *Phys. Rev. D* **82**, (2010) 123512 [arXiv:1008.1997 [hep-ph]];
- [3] A. Belyaev, M. T. Frandsen, F. Sannino and S. Sarkar, *Phys. Rev. D* **83**, (2011) 015007 [arXiv:1007.4839].
- [4] K. Petraki, L. Pearce and A. Kusenko, *JCAP* **07** (2014), 039 doi:10.1088/1475-7516/2014/07/039 [arXiv:1403.1077 [hep-ph]].
- [5] J. L. Feng, M. Kaplinghat, H. Tu and H. B. Yu, *JCAP* **07** (2009), 004 doi:10.1088/1475-7516/2009/07/004 [arXiv:0905.3039 [hep-ph]].
- [6] P. Agrawal, F. Y. Cyr-Racine, L. Randall and J. Scholtz, *JCAP* **1708** (2017) 021 doi:10.1088/1475-7516/2017/08/021 [arXiv:1702.05482 [astro-ph.CO]].
- [7] P. Agrawal, F. Y. Cyr-Racine, L. Randall and J. Scholtz, *JCAP* **05** (2017), 022 doi:10.1088/1475-7516/2017/05/022 [arXiv:1610.04611 [hep-ph]].
- [8] M. Cirelli, P. Panci, K. Petraki, F. Sala and M. Taoso, *JCAP* **05** (2017), 036 doi:10.1088/1475-7516/2017/05/036 [arXiv:1612.07295 [hep-ph]].
- [9] A. Sommerfeld, *Ann. Phys.* **403** (1931) 257-330
- [10] A. Abudurusuli and H. Iminniyaz, [arXiv:2001.08404 [hep-ph]].
- [11] J. L. Feng, M. Kaplinghat and H. B. Yu, *Phys. Rev. D* **82** (2010) 083525 doi:10.1103/PhysRevD.82.083525 [arXiv:1005.4678 [hep-ph]].
- [12] J. Chen and Y. F. Zhou, *JCAP* **1304** (2013) 017 doi:10.1088/1475-7516/2013/04/017 [arXiv:1301.5778 [hep-ph]].

- [13] N. Arkani-Hamed, D. P. Finkbeiner, T. R. Slatyer and N. Weiner, Phys. Rev. D **79** (2009), 015014 doi:10.1103/PhysRevD.79.015014 [arXiv:0810.0713 [hep-ph]].
- [14] M. Pospelov and A. Ritz, Phys. Lett. B **671** (2009), 391-397 doi:10.1016/j.physletb.2008.12.012 [arXiv:0810.1502 [hep-ph]].
- [15] J. D. March-Russell and S. M. West, Phys. Lett. B **676** (2009), 133-139 doi:10.1016/j.physletb.2009.04.010 [arXiv:0812.0559 [astro-ph]].
- [16] T. Bringmann and S. Hofmann, JCAP **0704** (2007) 016 Erratum: [JCAP **1603** (2016) E02] doi:10.1088/1475-7516/2007/04/016, 10.1088/1475-7516/2016/03/E02 [hep-ph/0612238].
- [17] T. Bringmann, New J. Phys. **11** (2009) 105027 doi:10.1088/1367-2630/11/10/105027 [arXiv:0903.0189 [astro-ph.CO]].
- [18] B. von Harling and K. Petraki, JCAP **12** (2014), 033 doi:10.1088/1475-7516/2014/12/033 [arXiv:1407.7874 [hep-ph]].
- [19] S. Cassel, J. Phys. G **37** (2010), 105009 doi:10.1088/0954-3899/37/10/105009 [arXiv:0903.5307 [hep-ph]].
- [20] T. R. Slatyer, JCAP **02** (2010), 028 doi:10.1088/1475-7516/2010/02/028 [arXiv:0910.5713 [hep-ph]].
- [21] M. L. Graesser, I. M. Shoemaker and L. Vecchi, JHEP **1110**, (2011) 110 [arXiv:1103.2771 [hep-ph]].
- [22] H. Iminiyaz, M. Drees and X. Chen, JCAP **1107**, (2011) 003 [arXiv:1104.5548 [hep-ph]].
- [23] R. J. Scherrer and M. S. Turner, Phys. Rev. D **33**, (1986) 1585, Erratum-ibid. D **34**, (1986) 3263.
- [24] X. l. Chen, M. Kamionkowski and X. m. Zhang, Phys. Rev. D **64** (2001), 021302 doi:10.1103/PhysRevD.64.021302 [arXiv:astro-ph/0103452 [astro-ph]].
- [25] S. Hofmann, D. J. Schwarz and H. Stoecker, Phys. Rev. D **64** (2001), 083507 doi:10.1103/PhysRevD.64.083507 [arXiv:astro-ph/0104173 [astro-ph]].